

however, such mixing has been postulated in the reactions of Fe^+ .⁹

Summary

The reactions of Co^+ and Ni^+ with CH_3X ($\text{X} = \text{Cl}, \text{Br}, \text{I}$) are studied by using guided ion beam mass spectrometry. In all reactions, only two ionic products are observed, MX^+ and MCH_3^+ . $D^\circ(\text{M}^+-\text{CH}_3)$ values for $\text{M} = \text{Co}$ and Ni are derived in each of the systems. These bond strengths agree well with our earlier determinations from alkane studies, but the CoCH_3^+ bond energy conflicts with other literature values. In addition, M^+-Cl bond energies are determined for both metals from the reaction with CH_3Cl . Previous values for the MCl^+ bond strengths are not available for comparison. The $\text{IP}(\text{NiCl})$ value determined here, however, differs by >2 eV from an earlier reported value which is clearly in error.

The reaction of $\text{Co}^+ + \text{CH}_3\text{I}$ forms CoCH_3^+ via both an exothermic and endothermic pathway. We explain this as due to

(38) Loh, S. K.; Fisher, E. R.; Lian, L.; Schultz, R. H.; Armentrout, P. B. *J. Phys. Chem.* 1989, 93, 3159-3167.

electronic state effects; i.e., the $\text{Co}^+(^5\text{F})$ first excited state reacts very efficiently and exothermically with methyl iodide, while the $\text{Co}^+(^3\text{F})$ ground state reacts endothermically. This behavior is successfully modeled here and explains why we reach different thermochemical conclusions for $D^\circ(\text{Co}^+-\text{CH}_3)$ than those obtained by Allison and Ridge from ICR studies of the same reactions.¹⁻³

Two reaction mechanisms are proposed that explain dual features seen in the formation of MX^+ . At low energies, an intermediate complex is formed by insertion of the metal ion into the C-X bond of CH_3X . This then leads to MCH_3^+ and MX^+ formation. At high energies, a direct mechanism in which the incident ion interacts primarily with the halide atom accounts for a second feature in the MX^+ cross section.

Acknowledgment. This work was funded by the National Science Foundation, Grant CHE-8796289. E.R.F. thanks David A. Hales and Dr. Mary Ellen Weber for their help in performing these experiments.

Registry No. Co^+ , 16610-75-6; Ni^+ , 14903-34-5; CH_3Cl , 74-87-3; CH_3Br , 74-83-9; CH_3I , 74-88-4.

Guided Ion Beam Studies of the State-Specific Reactions of $\text{Fe}^+(^6\text{D}, ^4\text{F})$ with CH_3X ($\text{X} = \text{Cl}, \text{Br}, \text{I}$)

Ellen R. Fisher, Richard H. Schultz, and P. B. Armentrout*[†]

Department of Chemistry, University of Utah, Salt Lake City, Utah 84112 (Received: February 21, 1989)

Reactions of Fe^+ with CH_3X ($\text{X} = \text{Cl}, \text{Br}, \text{I}$) are studied by guided ion beam techniques. State-specific reaction cross sections for production of FeCH_3^+ and FeX^+ are presented for the ^6D ground and the ^4F first excited states of Fe^+ . The overall behavior seen in these reactions is similar to that seen in the analogous reactions of Co^+ and Ni^+ , discussed in the preceding paper in this issue. The two states of Fe^+ exhibit large differences in reactivity, with the ^4F state generally being more reactive than the ^6D state for production of FeX^+ and FeCH_3^+ . The only exception is for the exothermic formation of FeCH_3^+ below 0.7 eV in the CH_3I system. We postulate that this is due to a potential energy surface crossing that is avoided at low kinetic energies due to spin-orbit interactions and is permitted at higher energies. Analysis of the threshold behavior of the endothermic reactions provides two determinations of $D^\circ(\text{Fe}^+-\text{CH}_3) = 2.49 \pm 0.13$ and 2.47 ± 0.07 eV, in good agreement with previous values. Lower limits are placed on the bond energies for Fe^+-X .

Introduction

Several studies in our laboratory have been directed at elucidating thermodynamic and mechanistic information about transition-metal hydrides and alkyls in an attempt to determine state-specific reactivity as well as periodic trends in reactivity.¹ Investigation of the reactions of Fe^+ with molecular hydrogen revealed that the ^4F first excited state of Fe^+ is more than an order of magnitude more reactive than the ^6D ground state.² This behavior is easily explained by using simple molecular orbital arguments that can also rationalize the behavior of *all* of the first-row transition-metal ions. For Fe^+ , the significant difference between the ^6D ($4s3d^6$) and ^4F ($3d^7$) states is the occupancy of the 4s orbital. The occupied 4s orbital of the ground state leads to repulsive interactions with the filled σ_g orbital of the H_2 molecule. Thus, the ground state reacts inefficiently. The first excited state avoids this repulsion and therefore reacts efficiently via a direct process.²

This strong correlation between electronic state and reactivity of Fe^+ was also found to be true for the endothermic reactions of Fe^+ with small alkanes.³ For exothermic reactions of Fe^+ with propane, however, it is the ground state that is more reactive at low kinetic energies, although at higher kinetic energies, it is once again the first excited state that is more reactive. This behavior

has been attributed to a crossing between quartet and sextet surfaces which is avoided due to spin-orbit mixing at low kinetic energies but is permitted at higher energies.

In this paper, we extend these studies by using guided ion beam techniques to examine the reactions of Fe^+ with methyl chloride, methyl bromide, and methyl iodide. The kinetic energy dependent reaction cross sections are presented for both $\text{Fe}^+(^4\text{F})$ and $\text{Fe}^+(^6\text{D})$, and comparisons are made between the reactivity displayed by Fe^+ in these systems with that seen with H_2 and the small alkanes. In addition to the state-specific results, comparisons are also made between the reactions of Fe^+ with the methyl halides and the results of our study involving Co^+ and Ni^+ .⁴

Experimental Section

The ion beam apparatus used in these experiments has been described in detail elsewhere.⁵ Conditions for these experiments

(1) (a) Elkind, J. L.; Armentrout, P. B. *Inorg. Chem.* 1986, 25, 1078-1080. (b) Elkind, J. L.; Armentrout, P. B. *J. Phys. Chem.* 1987, 91, 2037-2045. (c) Armentrout, P. B.; Georgiadis, R. *Polyhedron* 1988, 7, 1573-1581.

(2) Elkind, J. L.; Armentrout, P. B. *J. Am. Chem. Soc.* 1986, 108, 2765-2767. Elkind, J. J.; Armentrout, P. B. *J. Phys. Chem.* 1986, 90, 5736-5745.

(3) Schultz, R. H.; Armentrout, P. B. *J. Phys. Chem.* 1987, 91, 4433-4435. Schultz, R. H.; Elkind, J. L.; Armentrout, P. B. *J. Am. Chem. Soc.* 1988, 110, 411-423.

(4) Fisher, E. R.; Sunderlin, L. S.; Armentrout, P. B. *J. Phys. Chem.*, preceding paper in this issue.

[†]NSF Presidential Young Investigator, 1984-1989. Alfred P. Sloan Fellow. Camille and Henry Dreyfus Teacher-Scholar, 1987-1992.

TABLE I: Literature Heats of Formation of 298 K (kcal/mol)^a

| species | $\Delta_f H^\circ$ | species | $\Delta_f H^\circ$ |
|-----------------|--------------------|--------------------|----------------------------|
| Fe | 99.3 ± 0.3 | I | 25.51 ± 0.01 |
| Fe ⁺ | 282.3 ± 1.8 | CH ₃ Cl | -19.57 ± 0.12 ^b |
| CH ₃ | 34.8 ± 0.2 | CH ₃ Br | -8.48 ± 0.12 ^b |
| Br | 26.74 ± 0.014 | CH ₃ I | 3.51 ± 0.31 ^b |
| Cl | 28.99 ± 0.004 | | |

^aAll values, except where noted are from: Chase, M. W., Jr., et al. *J. Phys. Chem. Ref. Data* **1985**, *14*, Suppl. 1 (JANAF Tables). Ion heats of formation are calculated using the convention that the electron is a monatomic gas. Values compared from the literature which use the "stationary electron" convention should be increased by 1.48 kcal/mol at 298 K. ^bPedley, J. B.; Naylor, R. D.; Kirby, S. P. *Thermochemical Data of Organic Compounds*, 2nd ed.; Chapman and Hall: London, 1986.

and data reduction procedures are discussed in detail in the companion paper which examines the analogous reactions with Co⁺ and Ni⁺.⁴ The production of iron ions is described below. For these experiments, the ⁵⁶Fe (91.66% natural abundance) isotope was used. Fe(CO)₅ (99.5%) is obtained from Alfa, stored cold, and used without further purification except for multiple freeze-pump-thaw cycles. CH₃Br (99.5%) is obtained from Matheson and CH₃Cl (99.5%) from Aldrich. The CH₃I (99.5%) is obtained from Aldrich and is stored cold with Cu to help prevent decomposition. All the methyl halide gases are used without further purification except for multiple freeze-pump-thaw cycles.

A detailed description of the thermochemical analysis used in these experiments is provided in the companion paper.⁴ Briefly, cross sections for the endothermic formation of FeCH₃⁺ from CH₃Cl and CH₃Br are analyzed by using eq 1 where $m = 0, 1,$ and 3.

$$\sigma(E) = \sigma_0(E - E_T)^n/E^m \quad (1)$$

Heats of formation used in deriving thermochemical results are given in Table I. Exothermic reaction cross sections are usually described by using the Langevin-Gioumouis-Stevens (LGS) model⁶

$$\sigma_{\text{LGS}} = \pi e(2\alpha/E)^{1/2} \quad (2)$$

where e is the electron charge, α is the polarizability of the neutral molecule, and E is the relative kinetic energy of the reactants. Many exothermic reaction cross sections follow this type of energy dependence, although deviations from this behavior are commonly seen.⁷ As we shall see, in fact, the LGS model provides an incomplete description of the reaction cross sections determined here since the methyl halides are polar molecules. LGS theory, however, does provide a reasonable starting point for comparison of reaction and collision cross section magnitudes, even in these reactions.

Ion Sources. The metal ions are produced by one of two methods. In the surface ionization (SI) source, Fe(CO)₅ is passed through a water-cooled inlet line into the evacuated source chamber. The vapor is directed at a rhenium filament which is resistively heated to 2300 ± 100 K as measured by optical pyrometry. The metal complex decomposes on the filament, and metal ions are produced by surface ionization of the resulting metal atoms. If we presume that the Fe atoms reach equilibrium at the filament temperature before desorption, the electronic-state distribution of the beam produced by SI should have a Maxwell-Boltzmann distribution, 78.3 ± 1.0% Fe⁺(⁶D) and 21.3 ± 1.0% Fe⁺(⁴F). Previous studies in our laboratory on other systems indicate that this is a reasonable assumption.⁸

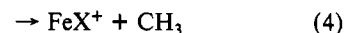
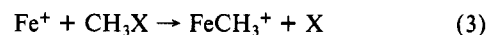
A second method of producing the metal ions takes Fe⁺ ions produced by electron impact ionization (EI) of Fe(CO)₅ and

focuses them into a high-pressure drift cell (DC). Ions are formed when the energy of the electron (E_e) exceeds the appearance potential of the metal ion from Fe(CO)₅ (14.2 ± 0.1 eV).⁹ At the Ees used (20–40 eV), sufficient energy is available to form excited states of Fe⁺. In the drift cell, the ions are thermalized by collisions with Ar or a mixture of Ar and O₂ at room temperature and pressures up to 300 mTorr. The ions drift to the exit of the cell under the influence of a weak electric field (0.5–3 eV). If there are greater than 600 collisions, relaxation of the excited ions to the ground state occurs. As discussed previously,² Fe⁺(DC) is believed to consist almost entirely of ground-state Fe⁺(⁶D) while Fe⁺(SI) contains ≈20% of the ⁴F first excited state.

Two tests are performed on the Fe⁺ ion beam to ensure that the Fe⁺ ions emerging from the DC are indeed in the ground state. First, we verify that reaction with D₂ yields results similar to those observed for Fe⁺(⁶D) from a previous study.² This test is a sensitive measure of the amount of Fe⁺(⁴F) present in the beam. As a second test, the ions are reacted with O₂ and the results are compared with those of our recent study,¹⁰ which revealed that higher excited states of Fe⁺ react efficiently with O₂ at low kinetic energies. Results shown here for Fe⁺(⁶D) pass both tests, thus assuring that the Fe⁺ ions produced in the drift cell are completely thermalized.

Results

The reaction of Fe⁺ with the methyl halides (X = Cl, Br, or I) yields two product channels, corresponding to reactions 3 and 4. No other ionic species (e.g., MH⁺, MCH₂⁺, MCHX⁺, or



MCH₃X⁺) are seen despite a careful search for these products.

Fe⁺(SI) and CH₃Cl. The ionic products observed in reactions 3 and 4 for Fe⁺(SI) and CH₃Cl are shown in parts a and b, respectively, of Figure 1. Reaction 3 is endothermic with an apparent threshold of about 1.6 eV. The cross section rises smoothly to a maximum of about 0.40 Å² at ≈3.6 eV, corresponding to the CH₃Cl dissociation energy, $D^\circ(\text{CH}_3\text{-Cl}) = 3.61$ eV. Beyond this energy, the cross section declines slightly, presumably due to the onset of dissociation to Fe⁺ + CH₃ + Cl.

The FeCl⁺ cross section has two distinct features (Figure 1b). At energies below 1.8 eV, the cross section is exothermic, decreasing as about 0.3σ_{LGS} at the lowest energies and as $E^{-1.9 \pm 0.1}$ from 0.3 to 1.5 eV. Above 1.8 eV, another feature appears that peaks at 4–5 eV (above the dissociation energy of CH₃Cl) and then decreases rapidly.

Although no new channels are observed, the reactivity of Fe⁺(DC) = Fe⁺(⁶D) with methyl chloride is significantly different from that observed with Fe⁺(SI) (Figure 1). For the FeCH₃⁺ product, cross-section magnitude is lowered by a factor of about 2.5, and the apparent threshold is raised by ~1.5 eV. The magnitude of σ(FeCl⁺) is also lowered considerably from the SI data. Thus the differences in reactivity between Fe⁺(SI) and Fe⁺(DC) reflect a larger reactivity for Fe⁺(⁴F). The conversion of the raw DC and SI data to the true state behavior is straightforward. At 2300 ± 100 K, the SI beam contains 78.3 ± 1.0% Fe⁺(⁶D) and 21.3 ± 1.0% Fe⁺(⁴F). To extrapolate to the true behavior of the Fe⁺(⁴F) excited state, the DC data (which is equivalent to pure ⁶D state Fe⁺) is scaled by a factor of 0.783 and subtracted from the SI data, and the remainder is divided by 0.213. The same procedure is used in all the reaction systems discussed below.

The results of such a calculation for the FeCH₃⁺ and FeCl⁺ products are also shown in Figure 1. For reaction 3, Fe⁺(⁶D) is less reactive than Fe⁺(⁴F) by a factor of ~6 above 4 eV and by even larger amounts at lower energies. Also, the maximum cross section for Fe⁺(⁶D) is only 0.15 Å² and occurs at about 6 eV, well

(5) Ervin, K. M.; Armentrout, P. B. *J. Chem. Phys.* **1985**, *83*, 166–189.

(6) Gioumouis, G.; Stevenson, D. P. *J. Chem. Phys.* **1958**, *29*, 292–299.

(7) Armentrout, P. B. In *Structure/Reactivity and Thermochemistry of Ions*; Ausloos, P., Lias, S. G., Eds.; Reidel: Dordrecht, 1987; pp 97–164.

(8) Sunderlin, L. S.; Armentrout, P. B. *J. Phys. Chem.* **1988**, *92*, 1209–1219.

(9) Distefano, T. *J. Res. Natl. Bur. Stand.* **1970**, *74A*, 233–238.

(10) Loh, S. K.; Fisher, E. R.; Lian, L.; Schultz, R. H.; Armentrout, P. B. *J. Phys. Chem.* **1989**, *93*, 3159–3167.

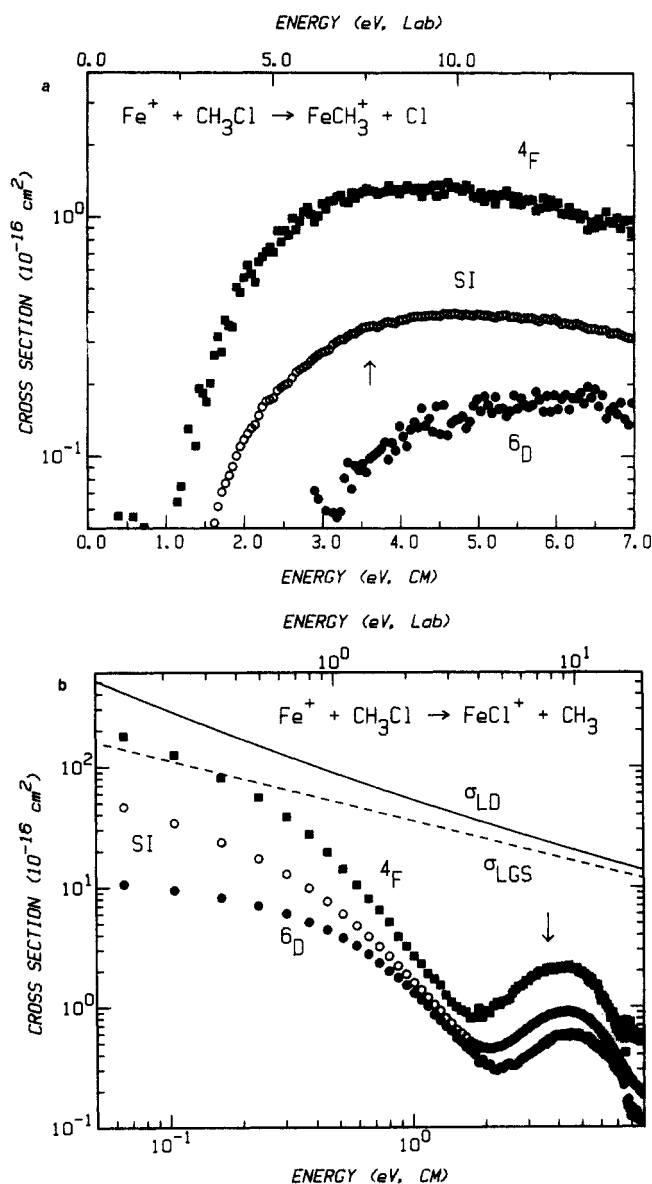


Figure 1. Cross sections for reactions 3 (part a) and 4 (part b) with CH_3Cl as a function of kinetic energy in the center-of-mass frame (lower scale) and laboratory frame of reference (upper scale). Open circles show results for Fe^+ produced in the SI source, closed circles represent $\text{Fe}^+(\text{6D})$ data, and closed squares are derived results for $\text{Fe}^+(\text{4F})$ (see text). The arrows indicate the neutral bond energy, $D^0(\text{CH}_3\text{Cl}) = 3.61$ eV. The dashed line (part b) shows the LGS cross section, eq 2, calculated with $\alpha(\text{CH}_3\text{Cl}) = 4.44 \text{ \AA}^3$. The solid line (part b) represents the locked dipole model cross section, eq 6, calculated using $\mu_D(\text{CH}_3\text{Cl}) = 1.87 \text{ D}$.

above $D^0(\text{CH}_3\text{-Cl})$. Reaction of the first excited state, however, reaches a maximum cross section of 1.3 \AA^2 at about 3.5–4.0 eV. This type of behavior is qualitatively similar to that observed in the endothermic reactions of Fe^+ with H_2 ,² methane, ethane, and propane.³ For reaction 4, $\text{Fe}^+(\text{4F})$ is 20 times more reactive than $\text{Fe}^+(\text{6D})$ at the lowest energies, while at higher energies, it is a factor of 4 times more reactive.

$\text{Fe}^+ + \text{CH}_3\text{Br}$. In the reaction of $\text{Fe}^+(\text{SI})$ with methyl bromide, reaction 3 is endothermic with an apparent threshold of about 0.7 eV; see Figure 2a. The cross section peaks about 4.0 eV, above $D^0(\text{CH}_3\text{-Br}) = 3.04$ eV. At higher energies, the cross section declines slightly. The FeBr^+ product cross section has two features (Figure 2b) similar to that of the FeCl^+ product. At the lowest energies, the cross section is exothermic, with a reaction efficiency of about $0.5\sigma_{\text{LGS}}$ below about 0.2 eV. At higher energies, the cross section decreases as $E^{-1.8 \pm 0.1}$. The second feature rises at about 2.0 eV, peaking at approximately 4 eV, well above the neutral bond energy.

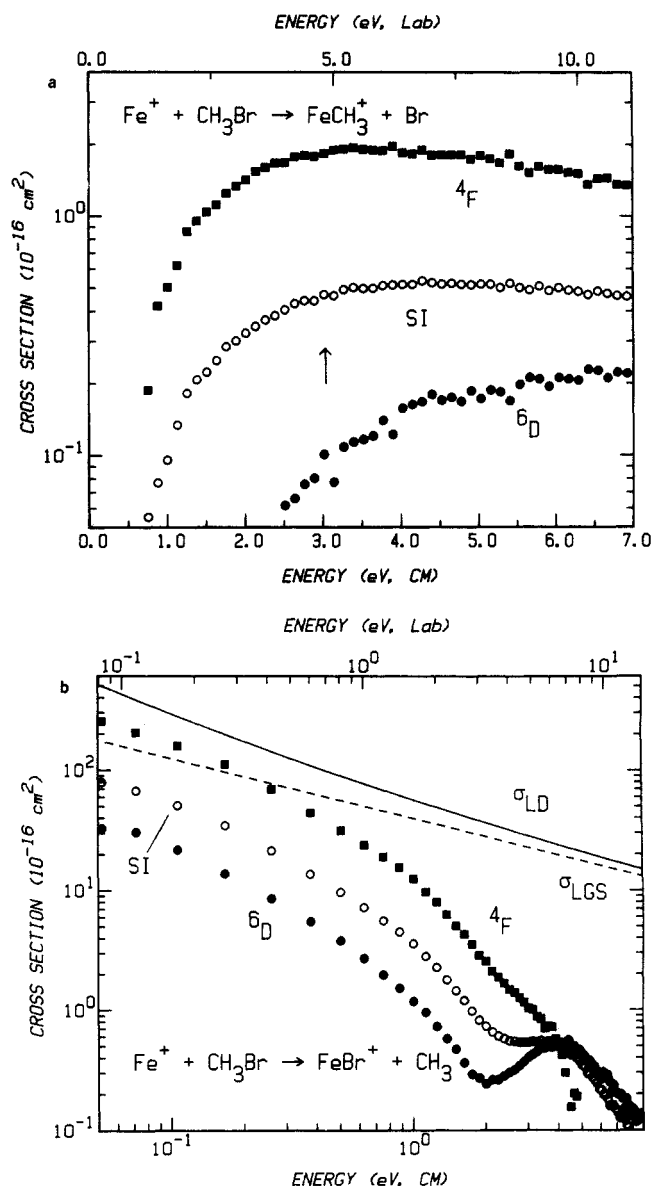


Figure 2. Cross sections for reactions 3 (part a) and 4 (part b) with CH_3Br as a function of kinetic energy in the center-of-mass frame (lower scale) and laboratory frame of reference (upper scale). Open circles show results for Fe^+ produced in the SI source, closed circles represent $\text{Fe}^+(\text{6D})$ data, and closed squares are derived results for $\text{Fe}^+(\text{4F})$ (see text). The arrows indicate the neutral bond energy, $D^0(\text{CH}_3\text{Br}) = 3.04$ eV. The dashed line (part b) shows the LGS cross section, eq 2, calculated with $\alpha(\text{CH}_3\text{Br}) = 5.44 \text{ \AA}^3$. The solid line (part b) represents the locked dipole model, eq 6, calculated with $\mu_D(\text{CH}_3\text{Br}) = 1.79 \text{ D}$.

As with methyl chloride, $\text{Fe}^+(\text{6D})$ reacts with CH_3Br to form FeCH_3^+ and FeBr^+ much less efficiently than $\text{Fe}^+(\text{4F})$ does. The apparent threshold for formation of FeCH_3^+ rises by about 1.8 eV. Also, the decrease in cross-section magnitude again reflects an order of magnitude difference in reactivity between $\text{Fe}^+(\text{6D})$ and $\text{Fe}^+(\text{4F})$ (Figure 2a). Much like the FeCl^+ product, the size of the FeBr^+ cross section from $\text{Fe}^+(\text{6D})$ is smaller than that from $\text{Fe}^+(\text{4F})$. At all energies, $\text{Fe}^+(\text{4F})$ is more reactive than $\text{Fe}^+(\text{6D})$, and below 0.2 eV, actually reacts with greater than LGS efficiency (Figure 2b).

$\text{Fe}^+ + \text{CH}_3\text{I}$. The cross sections for the products of reactions 3 and 4 for $\text{Fe}^+(\text{SI})$ and CH_3I are similar to each other in shape at low energies; see Figure 3. Formation of FeCH_3^+ , reaction 3, is exothermic, as evidenced by the increasing cross section at decreasing energies. At the lowest energies, the cross section magnitude is about $0.25\sigma_{\text{LGS}}$. Beginning ~ 0.3 eV, $\sigma(\text{FeCH}_3^+)$ decreases as $E^{-1.5 \pm 0.1}$ until ~ 2 eV, where it is nearly constant, decreasing slightly at energies higher than ~ 8 eV. The cross section for reaction 4 is larger than $\sigma(\text{FeCH}_3^+)$ at low energies,

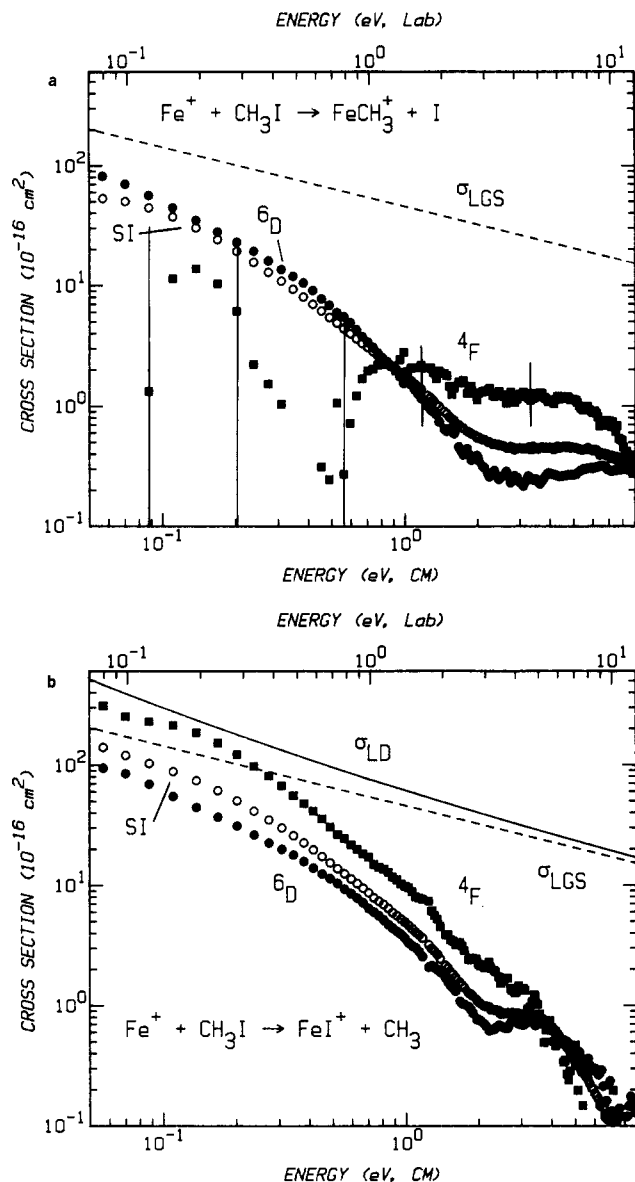


Figure 3. Cross sections for reactions 3 (part a) and 4 (part b) with CH₃I as a function of kinetic energy in the center-of-mass frame (lower scale) and laboratory frame of reference (upper scale). Open circles show results for Fe⁺ produced in the SI source, closed circles represent Fe⁺(DC) = Fe⁺(⁶D) data, and closed squares are derived results for Fe⁺(⁴F) (see text). The dashed lines show the LGS cross section, eq 2, calculated with $\alpha(\text{CH}_3\text{I}) = 7.29 \text{ \AA}^3$. The solid line in part b represents the locked dipole model, eq 6, calculated with $\mu_D(\text{CH}_3\text{I}) = 1.65 \text{ D}$. Vertical bars in part a show one standard deviation uncertainties in the derived cross sections for reaction of Fe⁺(⁴F).

and the $\sigma(\text{FeI}^+)$ has two distinct features. Reaction 4 is clearly exothermic and has a cross section of about $0.75\sigma_{\text{LGS}}$ at the lowest energies. The FeI⁺ cross section is relatively flat between 2 and 4 eV, decreasing rapidly beyond $\sim 5 \text{ eV}$.

The cross section for the FeCH₃⁺ product from Fe⁺(DC) is slightly greater in size than that from Fe⁺(SI) below about 0.8 eV. This indicates that the Fe⁺(⁶D) is at least as reactive as the Fe⁺(⁴F) at low energies. At higher energies, the cross section from the DC data is smaller than that from the SI data. Deriving the behavior of the excited state introduces a large uncertainty in the absolute size of the Fe⁺(⁴F) cross section at low energies since it involves subtracting two large numbers which have a small difference (Figure 3a). Despite this uncertainty, it seems clear that Fe⁺(⁴F) is less reactive than Fe⁺(⁶D) at energies below about 0.8 eV. Above 1.0 eV, Fe⁺(⁴F) is more reactive than the ground-state Fe⁺(⁶D). This type of behavior is similar to that observed previously for the exothermic reactions of Fe⁺ with propane.³

TABLE II: Reaction Rates at 298 K^a

| reaction | SI | ⁶ D | ⁴ F | AR ^b |
|---------------|----------------|----------------|--------------------|-----------------|
| (4) X = Cl | 3.1 ± 0.6 | 0.93 ± 0.2 | 8.6 ± 1.7 | |
| (4) X = Br | 9.4 ± 1.9 | 1.8 ± 0.4 | 38.0 ± 7.6 | |
| (3) X = I | 2.9 ± 0.6 | 3.7 ± 0.7 | $\sim 0.3 \pm 0.1$ | 1.9 |
| (4) X = I | 8.4 ± 1.7 | 5.6 ± 1.1 | 19.0 ± 5.8 | 1.9 |
| (3 + 4) X = I | 11.3 ± 2.3 | 9.3 ± 1.9 | 19.3 ± 5.8 | 3.8 |

^a Units of $10^{-10} \text{ cm}^3 \text{ s}^{-1}$, calculated from the data as described in ref 12. ^b Allison and Ridge. Values are from ref 11a.

TABLE III: Optimum Fitting Parameters^a

| reaction products | <i>n</i> | σ_0 | $E_T, \text{ eV}$ | $\text{av } E_T, \text{ eV}$ |
|-------------------------------------|---------------|---------------|-------------------|------------------------------|
| FeCH ₃ ⁺ + Cl | 1.9 ± 0.1 | 1.0 ± 0.3 | 0.88 ± 0.08 | 0.84 ± 0.10 |
| FeCH ₃ ⁺ + Br | 2.1 ± 0.2 | 1.1 ± 0.2 | 0.30 ± 0.07 | 0.29 ± 0.07 |
| FeCH ₃ ⁺ + I | | | <0.0 | |

^a Optimum values of parameters in eq 1 when $m = 1$. ^b Average value for all threshold analyses including forms where $m = 0, 1$, and 3.

For reaction 4 with X = I, Fe⁺(⁶D) is less reactive than Fe⁺(⁴F) by a factor of about 3. At higher energies, the difference in reactivity decreases, and the cross section resulting from reaction of Fe⁺(⁴F) decreases to approximately the same size as that from Fe⁺(⁶D).

Comparison to Previous Results. When Allison and Ridge (AR) studied the reactions of Fe⁺ with methyl halides by ion cyclotron resonance techniques,¹¹ they observed only FeBr⁺ from the reaction of Fe⁺ + CH₃Br but saw both FeCH₃⁺ and FeI⁺ in the CH₃I system. These results are entirely consistent with our observations at low kinetic energies. With CH₃I, AR report a total reaction rate of $(3.8 \pm 1.5) \times 10^{-10} \text{ cm}^3 \text{ s}^{-1}$.^{11a} We derive somewhat higher total reaction rates¹² for the same reactions for both ground state Fe⁺(⁶D) and the excited state Fe⁺(⁴F); see Table II. This table lists reaction rates for all of the exothermic reactions studied here.

For reaction with CH₃I, AR also report branching ratios for reactions 3 and 4. AR found FeCH₃⁺/FeI⁺ branching ratios of 52:48^{11c} and 50:50.^{11a} At thermal energies, we determine branching ratios of $26:74 \pm 10$ for Fe⁺(SI), $40:60 \pm 10$ for Fe⁺(⁶D), and $10:90 \pm 20$ for Fe⁺(⁴F). Since the data for the Fe⁺(⁴F) are more uncertain at the lowest energies, we report larger error limits for the excited-state branching ratio. The differences between the reaction rates and branching ratios determined here and those reported by AR may arise from the presence of different populations of electronic states of Fe⁺ in AR's and our experiments. AR produced Fe⁺ by EI on Fe(CO)₅, and although they note that the measured reaction rates are not dependent on the electron energy, experiments in our laboratories have shown that even electron energies as low as 25 eV can produce significant quantities of excited states of Fe⁺ above the ⁴F.^{2,10}

Discussion

Thermochemistry. The two endothermic reactions observed here (reaction 3 for CH₃Cl and CH₃Br) are analyzed by using eq 1. Detailed results for the $m = 1$ optimized fits to the data are given in Table III for these reactions. (Explicit consideration of the *J* levels as described for the Co⁺ and Ni⁺ systems⁴ yields identical results.) In both cases, the data for the derived Fe⁺(⁴F) reactions are examined. No analysis is attempted for the Fe⁺(⁶D) data because the endothermic cross sections are small and rise slowly from threshold, making accurate analysis difficult. The average E_T values given in Table III are averages of several different data sets using three fits ($m = 0, 1, 3$) for each data set. The cited uncertainties arise from the spread in these values and the uncertainty in the energy scale, and are the pooled estimate

(11) (a) Allison, J.; Ridge, D. P. *J. Organomet. Chem.* **1975**, *99*, C11–C14. (b) Allison, J.; Ridge, D. P. *J. Am. Chem. Soc.* **1979**, *101*, 4998–5009. (c) Allison, J.; Ridge, D. P. *J. Am. Chem. Soc.* **1976**, *98*, 7445–7447.

(12) Rate constants are derived from the cross sections at the lowest kinetic energies by using the formula $k(E) = \sigma v$, where v is the relative velocity of the reactants. See ref 5.

TABLE IV: Derived Bond Energies

| system | $D^{\circ}(\text{M}^+-\text{CH}_3)$ | $D^{\circ}(\text{M}^+-\text{X})$ |
|------------------------------------|-------------------------------------|----------------------------------|
| $\text{Fe}^+:\text{CH}_3\text{Cl}$ | 2.49 ± 0.13 | >3.61 |
| $\text{Fe}^+:\text{CH}_3\text{Br}$ | 2.47 ± 0.07 | >3.04 |
| $\text{Fe}^+:\text{CH}_3\text{I}$ | $>2.41 \pm 0.05$ | >2.46 |
| $\text{Fe}^+:\text{ethane}$ | 2.51 ± 0.10^a | |

^a Value from ref 3.

of error.¹³ All derived thermodynamic quantities are presumed to be at 298 K.

Bond energies for Fe^+-CH_3 are derived by using the formula $D^{\circ}(\text{Fe}^+-\text{CH}_3) = D^{\circ}(\text{X}-\text{CH}_3) - E_{\text{T}} - E_{\text{el}}$, where the electronic energy of the ^4F first excited state, E_{el} , is included since the analysis is for the ^4F state-specific data. At 2300 K, the average energy of the ^4F state is 0.284 eV. The results are given in Table IV. We also obtain a consistent lower limit to $D^{\circ}(\text{Fe}^+-\text{CH}_3)$ based on the exothermicity (i.e., $E_{\text{T}} \leq 0$) of reaction 3 in the CH_3I system for $\text{Fe}^+(^6\text{D})$. For this state, $E_{\text{el}} = 0.052$ eV for a completely statistical distribution according to the $2J + 1$ degeneracies. To account for possible nonstatistical distributions in the J levels due to quenching, we use $E_{\text{el}} = 0.05 \pm 0.05$ eV. The results from all three reactions are in excellent agreement with previous results from alkane studies in our laboratory,³ also shown in Table IV. We therefore recommend $D^{\circ}(\text{Fe}^+-\text{CH}_3) = 2.51 \pm 0.10$ eV, the value derived in the alkane study.³ In addition to the bond energies derived for the methyl products, lower limits have been set for the bond energies of the Fe^+-X species. The limits derived here are in agreement with previously determined limits on these values.¹¹

Exothermic Reactions. As noted in the Results, reaction of both the ground and first excited states of Fe^+ to form the iron halide ion product is exothermic with all three methyl halides. As can be seen in Figures 2b and 3b, the $\text{Fe}^+(^4\text{F})$ reacts with all three methyl halides with greater than LGS efficiency. The LGS theory, eq 2, fails to accurately describe the reaction cross sections in these reactions because it does not account for the permanent dipole moment of the methyl halide molecules. Several theories¹⁴⁻¹⁶ have been developed that provide a basis for understanding observed rate constants and cross sections for ion-polar molecule reactions.

Hamill and co-workers^{14,15} were among the first to treat the reaction between an ion and a polar molecule. They did so by adding the ion-permanent dipole potential, eq 5, to the charge-

$$V_{\text{D}} = (-e\mu_{\text{D}}/R^2) \cos \theta \quad (5)$$

induced dipole potential. Here, μ_{D} is the dipole moment of the molecule and θ is the angle the dipole makes with R , the ion-molecule separation. In the locked dipole (LD) model, the assumption is made that $\theta = 0$ in order to simplify the calculation. This assumption dictates that the neutral molecule is aligned in the lowest energy orientation with the dipole favorably directed along R . If the dipole orientation adjusts sufficiently rapidly as the encounter proceeds, then θ is always 0, $\cos \theta = 1$, and the largest possible cross section results. The LD model is physically unrealistic since the molecule will, in general, be rotating as it collides with the ion and will be unable to reorient itself rapidly enough to maintain $\theta = 0$. Nonetheless, the LD model is useful as an upper limit to the cross section for reaction between an ion and a polar neutral molecule. This maximum cross section can be calculated by use of eq 6. The energy dependence of σ_{LD}

$$\sigma_{\text{LD}} = \pi e(2\alpha/E)^{1/2} + \pi\mu_{\text{D}}e/E \quad (6)$$

changes from E^{-1} at low kinetic energies to $E^{-1/2}$, thus approaching the LGS model at higher kinetic energies.

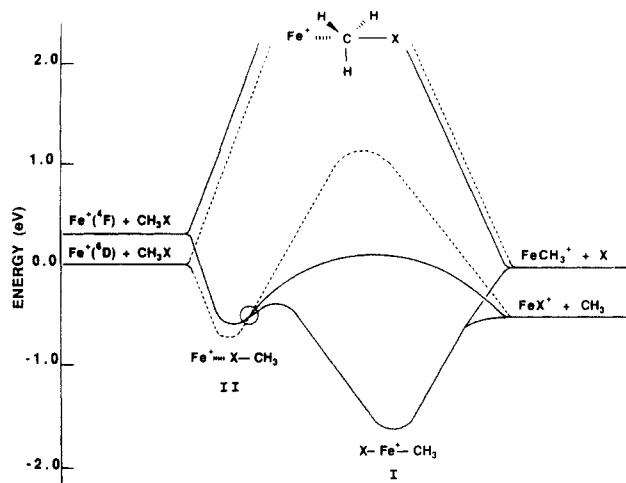


Figure 4. Qualitative potential energy surfaces for the reaction of Fe^+ with the methyl halides. Solid lines represent the quartet surfaces, while dashed lines show the sextet surfaces. The circle indicates the crossing between the two surfaces, which is avoided at low kinetic energies but permitted at high energies (see text). The relative energies of reactants and products correspond most closely to the CH_3I system.

The LD cross sections have been calculated for all three methyl halides by using eq 6 and the values $\alpha(\text{CH}_3\text{Cl}) = 4.44 \text{ \AA}^3$, $\mu_{\text{D}}(\text{CH}_3\text{Cl}) = 1.87 \text{ D}$, $\alpha(\text{CH}_3\text{Br}) = 5.44 \text{ \AA}^3$, $\mu_{\text{D}}(\text{CH}_3\text{Br}) = 1.79 \text{ D}$, $\alpha(\text{CH}_3\text{I}) = 7.29 \text{ \AA}^3$, and $\mu_{\text{D}}(\text{CH}_3\text{I}) = 1.65 \pm 0.2 \text{ D}$.¹⁷ These are shown in Figures 1b, 2b, and 3b. As can be seen in the figures at the lowest energies, the FeX^+ cross sections from $\text{Fe}^+(^4\text{F})$ fall between the predictions of the LGS model and the locked dipole theory. This is physically reasonable and an indication that the permanent dipole clearly must be accounted for in determining the collision cross sections at low energies.

Potential Energy Surfaces. The overall reaction mechanism for the reactions of Fe^+ with the methyl halides must be essentially the same as that for Co^+ and Ni^+ since the analogous ionic products are seen in these reactions and the overall behavior of the reaction products is similar for all three ions.⁴ With Fe^+ , however, our treatment of the qualitative potential energy surfaces (PESs) must explicitly include both the ground and first excited states of the ion. Previous studies^{2,3} have examined the different reactivities of $\text{Fe}^+(^6\text{D}, 4s3d^6)$ and $\text{Fe}^+(^4\text{F}, 3d^7)$ by using molecular orbital arguments.^{1-3,18,19} Briefly, we find that the different electron configurations of the two states lead to distinctly different PESs. The occupied $4s$ orbital of the ^6D state leads to strongly repulsive PESs which are evidenced by inefficient reactivity shifted to high energies.¹⁻³ Since the ^4F state has an empty $4s$ orbital, the PESs are more attractive and this state can react much more efficiently.

In the methyl halide systems, the PESs for the $\text{Fe}^+(^4\text{F})$ first excited state, Figure 4, are strictly analogous to those for the $\text{Co}^+(^3\text{F})$ and $\text{Ni}^+(^2\text{D})$ ground states⁴ since these three ions all have low-spin, $3d^n$ electron configurations. Experimental evidence for this comes from our observations that all of these ions react similarly with H_2 ^{1b} and with alkanes.^{3,20} Therefore, in analogy with the Co^+ and Ni^+ systems, we assume that the reactions can proceed at low energy via intermediates I, $\text{X}-\text{Fe}^+-\text{CH}_3$, and II, $\text{Fe}^+\cdots\text{X}-\text{CH}_3$, or at high energy via a more direct process that forms only FeX^+ . The $\text{Fe}^+\cdots\text{CH}_3-\text{X}$ approach is again very repulsive. We assume that the Fe^+-X and Fe^+-C bonds of I are full covalent bonds involving hybridized $s-d$ orbitals on the metal. This leaves five electrons that reside in four largely nonbonding $3d$ orbitals on the metal, such that I should have a quartet spin ground state. Thus, we postulate that diabatic formation of I from

(13) Box, G. E. P.; Hunter, W. G.; Hunter, J. S. *Statistics for Experimenters*; Wiley: New York, 1978; p 319.

(14) Theard, L. P.; Hamill, W. H. *J. Am. Chem. Soc.* **1962**, *84*, 1134-1138.

(15) Moran, T. F.; Hamill, W. H. *J. Chem. Phys.* **1963**, *39*, 1413-1422.

(16) Dugan, J. V., Jr.; Magee, J. L. *J. Chem. Phys.* **1967**, *47*, 3103-3112.
Su, T.; Bowers, M. T. *J. Chem. Phys.* **1973**, *59*, 3027-3037. Barker, R. A.; Ridge, D. P. *J. Chem. Phys.* **1976**, *64*, 4411-4416.

(17) Rothe, E. W.; Bernstein, R. B. *J. Chem. Phys.* **1959**, *31*, 1619-1627.

(18) Elkind, J. L.; Armentrout, P. B. *J. Phys. Chem.* **1985**, *89*, 5626-5636; *Ibid.* **1986**, *90*, 6576-6586; *J. Chem. Phys.* **1986**, *84*, 4862-4871.

(19) Elkind, J. L.; Armentrout, P. B. *J. Chem. Phys.* **1987**, *86*, 1868-1877.

(20) Georgiadis, R.; Fisher, E. R.; Armentrout, P. B. *J. Am. Chem. Soc.* **1989**, *111*, 4251-4262.

the $\text{Fe}^+(\text{}^4\text{F})$ and $\text{CH}_3\text{X}(\text{}^1\text{A}_1)$ reactants occurs with no barrier; see Figure 4.

For $\text{Fe}^+(\text{}^6\text{D})$, the initial approach of the neutral molecule is also attractive, again due to the long-range ion-permanent dipole attraction, but now the 4s orbital is occupied. Consequently, intermediate II occurs at a greater distance along the reaction coordinate and therefore lies in a potential well that is not as deep as for the $\text{}^4\text{F}$ PES. At still closer distances, the molecular orbital ideas alluded to above suggest that a fairly repulsive sextet surface results (Figure 4). Note that the quartet and sextet PESs must cross at some point along the reaction pathway, probably in the vicinity of the ion-dipole well.

The proposal that the sextet surface is much more repulsive than the analogous quartet surface can also be explained by viewing the reaction in reverse. If CH_3 approaches the metal end of MX^+ , intermediate I is formed only if the surface is low spin. (The repulsive high-spin surface is not shown in Figure 4.) If CH_3 approaches the halide end of MX^+ , there are no unpaired electrons available for bonding on the halide such that the interaction is anticipated to be repulsive for both the sextet and quartet surfaces. In order to follow the sextet surface back to $\text{Fe}^+(\text{}^6\text{D})\cdots\text{X}-\text{CH}_3$, the CH_3 must be high-spin coupled to the nonbonding 3d electrons on the $\text{Fe}^+(\text{}^6\text{D})$. In contrast, in order to produce $\text{Fe}^+(\text{}^4\text{F})\cdots\text{X}-\text{CH}_3$, the CH_3 must be low-spin coupled with the nonbonding 3d electrons on the metal ion. Low-spin coupling leads to a less repulsive surface for the $\text{Fe}^+(\text{}^4\text{F})$. Similar arguments have also been made for impulsive $\text{M}^+ + \text{H}_2$ interactions.^{1b,19}

Now consider the CH_3Cl reaction system. Formation of FeCH_3^+ is much more favorable for the $\text{}^4\text{F}$ state, Figure 1a, consistent with the spin-allowed formation of I. The $\text{Fe}^+(\text{}^6\text{D})$ cross section exhibits behavior characteristic of an inefficient impulsive process,^{2,3} in which the threshold for reaction is shifted to considerably higher energies. Such behavior is typical for repulsive PESs. For the FeCl^+ product (Figure 1b) the $\text{}^4\text{F}$ cross section is again much larger than that for the $\text{}^6\text{D}$ at all energies. As in the Co^+ and Ni^+ systems, we attribute the exothermic reactivity to a reaction mechanism that proceeds via intermediate I, while the high-energy feature is due to a more direct mechanism. Both of these processes are more favorable for the $\text{}^4\text{F}$ state. Indeed the high-energy feature in the $\text{}^6\text{D}$ cross section is shifted to somewhat higher energies, again consistent with a more repulsive PES. To explain the exothermic reactivity of the $\text{}^6\text{D}$ state within the context of the PESs of Figure 4, it is necessary to propose that $\text{Fe}^+(\text{}^6\text{D})$ can form I at low kinetic energies. This must involve a coupling of the quartet and sextet surfaces, presumably due to spin-orbit mixing. Such coupling is not without precedent since a similar proposal was needed to understand the state-specific reactivity in the exothermic reactions of Fe^+ with propane.³ The results of Figure 1b suggest that this coupling is largely inefficient since the $\text{}^4\text{F}$ is more reactive than the $\text{}^6\text{D}$ at all energies.

In the CH_3Br system, the state-specific results for reaction 3, Figure 2a, are very similar to those in the CH_3Cl system. Comparable results are also obtained for reaction 4, Figure 2b, *except* that there is no high-energy feature for the $\text{}^4\text{F}$ state. This could be because the barrier associated with the direct mechanism for FeBr^+ formation lies *below* the $\text{Fe}^+(\text{}^4\text{F}) + \text{CH}_3\text{Br}$ reactant energy (while in the CH_3Cl system and all the Co^+ and Ni^+ systems the barrier is above the reactant energies). Thus, formation of FeBr^+ from the $\text{}^4\text{F}$ state has no barrier whether formed via I or via the direct pathway.

In the CH_3I system, the FeI^+ cross sections, Figure 3b, behave similarly to the FeBr^+ results and can be explained analogously; however, the state-specific behavior for FeCH_3^+ formation is clearly distinct (Figure 3a). This reaction is now exothermic, and at low energies, it is the $\text{}^6\text{D}$ ground state that is more reactive than

the $\text{}^4\text{F}$ first excited state. At higher energies (above 0.8 eV), the relative reactivity returns to that observed for the endothermic formations of FeCH_3^+ in the CH_3Cl and CH_3Br systems.

A similar switch in state-specific reactivity is also seen in the exothermic reactions of Fe^+ with propane³ and is believed to be the result of the avoided crossing between the quartet and sextet PESs discussed earlier. We believe that the observed behavior in the exothermic FeCH_3^+ channel occurs because at low energies, the crossing is avoided most of the time such that $\text{Fe}^+(\text{}^6\text{D})$ correlates along an "adiabatic" PES to intermediate I, the only thermodynamically allowed pathway to formation of FeCH_3^+ . As the kinetic energy is increased, the crossing becomes increasingly less avoided until the system behaves diabatically, and it is the $\text{Fe}^+(\text{}^4\text{F})$ ion that correlates to intermediate I and from there to the FeCH_3^+ product.

The observation that the $\text{}^4\text{F}$ state reacts more efficiently than the $\text{}^6\text{D}$ state to form FeI^+ even at low energy is not inconsistent with the above explanation. For reaction of $\text{Fe}^+(\text{}^6\text{D})$ at low energies, the surface crossing is avoided such that I is formed. This then decomposes to give both FeI^+ and FeCH_3^+ , with the former favored 60:40. For $\text{Fe}^+(\text{}^4\text{F})$, the avoided crossing means that I is generally not formed at low energies, so that the only thermodynamically feasible reaction is formation of FeI^+ via the direct mechanism. Now the branching ratio favors FeI^+ by about an order of magnitude.

Summary

Guided ion beam mass spectrometry is used to study the state-specific reactions of $\text{Fe}^+(\text{}^6\text{D}, \text{}^4\text{F})$ with the methyl halides. It is found that the $\text{Fe}^+(\text{}^4\text{F})$ first excited state is much more reactive than the $\text{Fe}^+(\text{}^6\text{D})$ ground state in the endothermic formations of FeCH_3^+ from CH_3Cl and CH_3Br . This is despite its being only 0.25 eV higher in energy. In this respect, these reactions are much like the state-specific reactions of Fe^+ with H_2 and small alkanes. With CH_3I , however, the results are more complex, in part because formation of FeCH_3^+ is exothermic. Here, this reaction is more efficient for the $\text{}^4\text{F}$ state than for the $\text{}^6\text{D}$ state at energies above about 0.8 eV; it is the ground state that is more reactive below this energy. This difference in behavior is attributed to an avoided (but not entirely) crossing of quartet and sextet surfaces similar to that seen for the exothermic reactions of Fe^+ with propane.³ At low kinetic energies, spin-orbit coupling allows the reactants to follow the adiabatic PESs. At high kinetic energies, spin-orbit interactions become less important, the crossing is permitted, and diabatic behavior is seen.

Formation of FeX^+ is exothermic for all CH_3X studied here. Unlike the exothermic FeCH_3^+ product, there is no switch in reactivity between the two states of Fe^+ . The $\text{Fe}^+(\text{}^4\text{F})$ is more reactive than $\text{Fe}^+(\text{}^6\text{D})$ at all energies. The presence of two features in the FeCl^+ product is explained by two different mechanisms contributing to the formation of FeCl^+ , analogous to the results for Co^+ and Ni^+ reacting with all three methyl halides.⁴ At low energies, an intermediate complex is formed by insertion of the metal ion into the C-X bond. At higher energies, the reactants must overcome a barrier to form FeCl^+ via a direct pathway for both the $\text{}^4\text{F}$ and $\text{}^6\text{D}$ states. In the CH_3Br and CH_3I systems, the high-energy feature appears only for $\text{Fe}^+(\text{}^6\text{D})$. We speculate that in these systems the barrier to the direct mechanism is below the reactant energy for the $\text{}^4\text{F}$ state such that only exothermic formation of FeX^+ is observed and the high-energy feature disappears.

Acknowledgment. This work was funded by the National Science Foundation, Grant CHE-8796289.

Registry No. Fe^+ , 14067-02-8; CH_3Cl , 74-87-3; CH_3Br , 74-83-9; CH_3I , 74-88-4.